Computer-AidedDesign

Taylor & Francis
Taylor & Francis Group

Designing 3D tangible interfaces for understanding complex big data

Wen Qi [a] and Jean-Bernard Martens [b]

[a]Donghua University, China; [b]Technical University Eindhoven, Netherlands

ABSTRACT

Understanding big and complex scientific data is still an immature topic. It involves studying visualization methods to faithfully represent data, on the one hand, and designing interfaces that truly assist users with data analysis, on the other hand. In an earlier study, we developed guidelines for choosing display environment for four specific, but common, data analysis tasks: identification and judgment of the size, shape, density, and connectivity of objects in a volume. The results showed that using the fish tank virtual reality (VR) system was significantly more accurate at judging the shape, density, and connectivity of objects and significantly faster than the immersive Head-mounted display VR system. Based on those results, we asked the question whether or not the user performance could be further improved by adding tangible elements into the fish tank VR system. We propose several different interface prototypes of a clipping plane that have been realized with the help of wireless vision-based tracking. These prototypes allow to experience and evaluate those user interface strategies for performing the clipping plane function. An experimental study is carried out to quantitatively measure the added value of these tangible interfaces. The result shows that the inclusion of a tangible frame for controlling a virtual clipping plane and the correspondent 2D intersection image into the basic fish tank VR system significantly improve the user performance for the shape, size and the connectivity task.

1. Introduction

Developing user interfaces for portraying and interacting with large quantities of data to facilitate data analysis is rapidly becoming one of the most challenging topics in both HCI and visualization research areas[2,14,19]. Currently, the dominant interface for 3D manipulation with volumetric data is the computer desktop with a graphical user interface that is controlled by a mouse and keyboard. Researchers are also trying to tackle this interaction problem from the perspective of creating better interfaces, which refers to designing 3D VR system or adding tangible elements into 3D input devices.

Our study on 3D interface starts from the scientific problems asked by domain experts that are studying the structure of human lung mucus in both normal wild-type lungs and in the lungs of Cystic Fibrosis (CF) patients. This mucus is made up of a number of long polysaccharide molecules called mucins, and it is known that there are a number of different types of mucin present in the mucus, and that the mucus is denser for CF patients than wild-type mucus. What is not known is how the different types of mucin are distributed in the mucus, and how particles can diffuse through it. The mucins may be uniformly distributed, or form distinct domains. There may be web-like superstructures formed by a subset of the mucins which contain clumps of other mucins. There may be large, small, or a variety of different sized water pockets surrounded by thin membranes. Researchers are probing this by developing fluorescent dyes that attach differentially to the different mucin types, and by scanning the mucus with a confocal microscope to produce multiple 3D scalar fields, one for each dye. We wish to display the resulting scalar fields in 3D to help them estimate sizes, distributions, and shapes of any resulting voids and structural elements. A virus, bacteria, or bacterial colony would traverse the mucus differently depending on its structure. The motion of such pathogens is of great interest to the study of CF, because lung infections are the source of many CF deaths. Researchers are probing this by placing small beads of various radii into the mucus and tracking the Brownian-driven motion of these beads over time to understand how they move through the mucus matrix. We wish to display the resulting motion paths in the presence of the above mesh structure to help our users correlate structure and density with bead motion paths.

CONTACT Wen Qi ✉ design_wqi@sina.com

An earlier user study was designed to look into which type of VR interface is most suitable for those data analysis tasks discussed above [12]. The results indicated that an immersive VR environment without overview capability did not help users with most of the tasks (identifying the data structure and properties). The desktop VR environment helped users achieve better performance in terms of accuracy and the response time. But still the absolute performance is not very satisfying. Naturally, we ask whether there are other means that could further improve the user performance within such environment. We investigate whether or not the inclusion of a tangible interface and two handed interaction with such interface can help users perform these tasks better.

2. Related work

Many 3D interfaces that are based on advanced tracking technologies provide the possibilities of improving the 3D interaction process [5,7,16], and several studies have already been undertaken to develop alternative tangible interfaces for this purpose [13]. The Passive Interface Props (PassProps) [6] was one of the first 3D interfaces to support continuous clipping interaction in 3D space. The PassProps contains a head prop, a cutting plane prop for creating intersections, and a pen-like prop for planning trajectories. The head prop is used to manipulate the orientation of the patient's anatomy. The user holds the cutting-plane prop relative to the head prop to specify the location and orientation of the slice through the 3D data. The generated intersection image is presented on the display, next to a (volume) rendering of the 3D model.

De Guzman et al. presented two tangible devices for navigating a slice through the human body [3]. Interface A consisted of a 30-inch 2D model of a human body, together with a U-shaped fork at the end of an adjustable arm that could be rotated 180 degrees along the device's baseboard. Interface B consisted of a transparent 3D model of a human body and a free-moving handheld fork. The fork in each case represented the intersection plane (window), and its position and orientation was used to generate an intersection image on a separate display.

The Cubic Mouse (CMouse) [4] was developed to support exploration of 3D geological data (seismic data) and car crash data. The CMouse allows users to specify three orthogonal cutting planes and to perform so-called "chair cuts" through the data. The prop is a cube-shaped case with three perpendicular rods passing approximately through the centers of two parallel faces of the case. The rods are used to control three orthogonal slices through the 3D data, i.e., by pushing or pulling a rod, usually with the dominant hand, the corresponding intersection plane moves back and forth.

ActiveCube is another user interface which allows users to construct and interact with 3D environments using physical cubes equipped with input/output devices [10]. Spatial, temporal and functional consistency is always maintained between the physical object and its corresponding representation in the computer. This cube is equipped with three gyroscopic sensors and measures 3D orientation. It can measure relative angles around X, Y and Z coordinate axes with 8 bit resolution. A user can change the angle of the object by changing the angle of the constructed structure. Xu et al. [8,9,18] proposed a framework of processing multimedia resources.

3. User study

The study in this paper compares five different setups of tangible interface within the same baseline system: outside-in non-immersive desktop VR. The relative performances of these configurations are compared with each other for four generic tasks required in the analysis of high density volumetric data. The experimental setup for this study is described in the following section.

3.1. Apparatus

For the purpose of the user study with real-time performance, the hardware setup is organized around two Dell graphics workstations with different specific interface components. The first workstation is mainly used for tracking the tangible interface. It consists of the following components:

- One *DELL* Precision 530 workstation (Pentium IV, 2.4 GHz, 512 MB RAM) with ATI FireGL 4 graphics card coupled to an infrared emitter from *Stereo Graphics*.
- Two analog Leutron Vision LV-8500 progressive scan CCD cameras (720×576 pixels, 50 Hz frame rate) with COSMICAR/PENTAX lenses with a focal length of 12 mm and infrared transparent filters (that block visible light); these cameras are connected to two synchronized Leutron Vision Pict-Port H4D frame grabbers.
- A 14′ CRT monitor.

The second workstation includes the following components:

- One *DELL* Precision 670 workstation (Intel Xeon, Dual CPU, 3.2 GHz, 2.0 GB RAM) with NVidia Quadro FX 4500 graphics card.

- A 14′ CRT monitor from *DELL* with a vertical refresh rate up to 120 Hz, so that stereoscopic images can be viewed with the help of active liquid crystal shutter glasses (CrystalEyes 3).
- A 15′ LCD display from *DELL*.

The volume rendering algorithm is achieved with hardware-supported 3D texture mapping in OpenGL. The algorithm that renders the non-polygonal isosurfaces in the data set is based on the approach proposed by Westermann and Ertl [17]. The 3D image on the display is the result of volume rendering for a fixed virtual camera position that is behind the actual observer's viewpoint. The image changes in accordance with the movement of the tangible cube. The user needs to work with the tangible interfaces in his/her comfortable position while the objects in the experimental volume are shown with their reasonable sizes in the center of the screen.

3.2. Data and task

Simulated volumetric data are generated to act as trials in this study. A random number of two to four types of differently-shaped objects (sphere, ellipsoid, cylinder, and curved tube) are inserted with random positions into a rectangle volume. These objects may overlap with each other to become connected. The objects' properties (size, shape) and the volume density form experimental conditions that vary between trials. The bounding box of the volume is positioned in the center of a cube and subdivided into equally-sized eight subregions (a $2 \times 2 \times 2$ array in the x, y, and z directions) within which object density may differ. Subregions are labeled with unique numbers (1 through 8) to enable subjects to identify them.

There are always spheres and at least one curved tube within every trial volume. Trials may also contain ellipsoids, cylinders, and up to three additional curved tubes. Sphere sizes may vary between four possible radii in the range from six to twelve OpenGL units. The density of objects within each subregion is controlled to be sparse, medium, or dense. A single dense region (the "densest" region) exists within each volume. Sparse regions contain between 10%–60% of the number of objects in the dense region, while medium regions contain between 60%–90% of this number. Subjects are asked to provide their answers as accurately as possible and to minimize response time. The size, density, and curve counting questions are presented in a multiple choice format. Subjects are asked to describe the name of each kind of object for the shape question and to specify the subregion numbers for the tube tracking question. All the answers from the subjects are recorded by the experimenter on the answer sheets.

3.3. Experimental procedure

A between-subject design was used, with interface type as an independent factor:

1. Condition 1 (abbreviated as cube or C): baseline system is a non-immersive VR system with a tangible cube to orient the data set. The only visual feedback is the 3D image of the data set (Fig. 2);
2. Condition 2 (abbreviated as fixed-plane or CF): baseline system with a fixed virtual clipping plane. A user can manipulate the cube and cut through the data using a fixed clipping plane (Fig. 3a). The fixed virtual plane is in a position that is parallel to the vertical axis;
3. Condition 3 (abbreviated as tangible-frame or CT): baseline system with a tangible frame in the shape of clipping plane. The movement of the visual clipping plane corresponds to the physical plane shaped object. The visual feedbacks consist of the 3D representation of the data set and the virtual clipping plane on the screen (Fig. 1a);
4. Condition 4 (abbreviated as fixed-intersection or CFI): the interaction devices are the same as in condition 2. However, the visual feedbacks consists of the 3D rendering result and a synchronized 2D intersection image in a separate window (Fig. 3a and b);
5. Condition 5 (abbreviated as tangible-intersection or CTI): the interaction devices are the same as in condition 3. However, the visual feedbacks consist of both the 3D rendering result and a synchronized 2D intersection image in another window (Fig. 1a and b).

The proposed interface prototypes have been realized with the help of wireless vision-based tracking [15]. Subjects are randomly assigned into one of five groups. Subjects completed several steps during the experiment. As part of an initial interview session, they signed a consent form, answered basic demographic questions (age, gender, and occupation or major field of study), and identified their frequency of computer use and prior experience with any kind of VR and 3D visualization system. In a training session, the equipment is introduced and the tasks to be performed are described. Next, the formal experiment session was conducted. Each experiment included 11 trials, with each trial containing a single volumetric data set. These eleven data sets were indeed different from one another, and varied by object property (type, size, position) and volume density. However, the same set of trials (11 data sets) in the same order was used for all five groups (cube, fixed-plane,
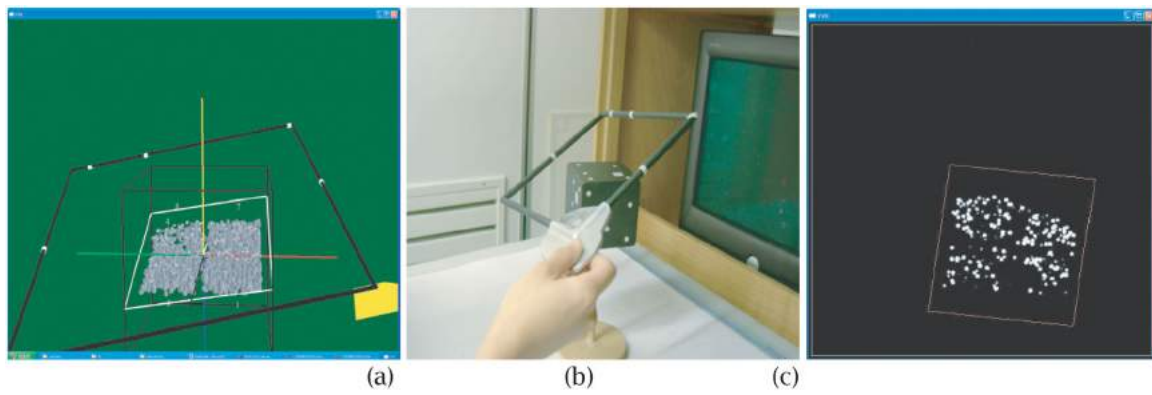
Figure 1. The diagram of condition 3 and condition 5: condition 3 includes (a) + (b); condition 5 also includes (c).
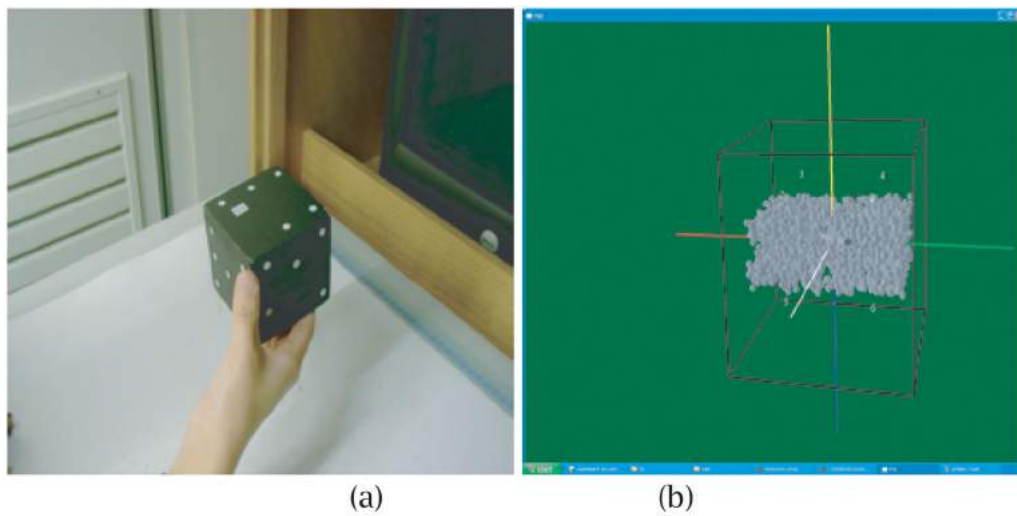

Figure 2. The diagram of condition 1, where the rendered volume follows the position and orientation of the physical cube.
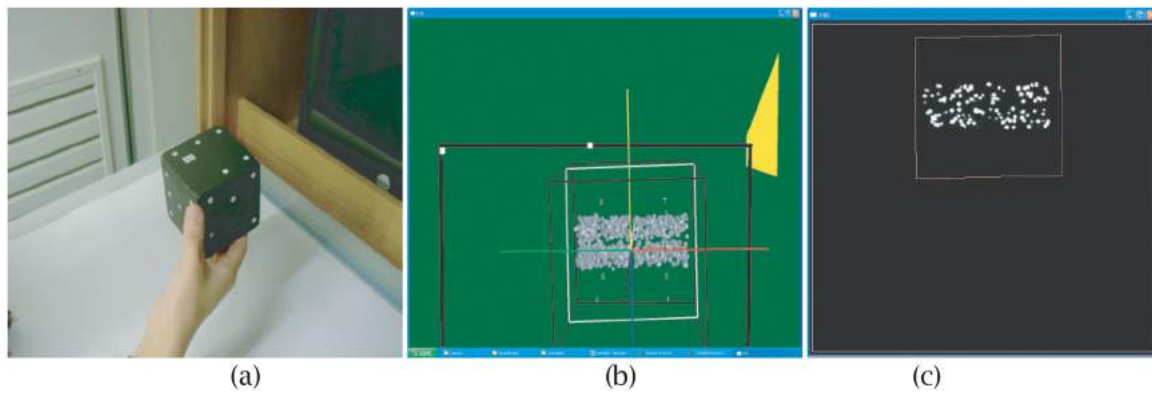

Figure 3. The diagram of condition 2 and condition 4: condition 2 includes (a) and (b); condition 4 also includes (c).

tangible-frame, fixed-intersection, and tangible intersection). A short break was provided every half hour or whenever a subject asked for one. After completing the last trial in the formal experiment session, subjects filled out a questionnaire describing their preferences, any suggestions they had on how to improve the system, and so on. The study ended with a short debriefing during which the experimenter summarized the study goals.

4. Results

25 subjects volunteered for our experiment, 11 males and 14 females. The subjects were randomly assigned into one of the five test groups: 5 subjects per group. The age of each subject and the frequency of computer use were recorded before the experiment and suggested we had similar ages and computer experience within each group. Two measures of performance were recorded for each trial a subject completed: response time rt and error rate Pe. A single rt value representing the total time in seconds needed to complete all four tasks was captured for each trial. We did not record the individual rt for each task since it is difficult to record separately. Four separate Pe values for four tasks that subjects completed were generated.

- For the shape, size, density and numberosity questions, the way to code the answers is 1 for correct and 0 for incorrect. Error rate Pe is the proportion of wrong answers among all the answers;
- For the connectivity question, subjects' answers were coded as two parameters: the false negative and the false positive used in a Receiver Operating Characteristic curve (ROC). Further analyses are based on these two parameters.

For rt statistics, trials were divided by interface system (cube, fixed-plane, or tangible-frame, fixed-intersection and tangible intersection). For Pe statistics, trials were divided by interface (cube, fixed-plane, or tangible-frame, fixed-intersection and tangible-intersection) and task (shape, size, density, or connectivity). The response time rt needed to complete a trial during each trial was recorded during the formal experiment session. Average time were $rt = 268.5$ s, 267.1 s, 244.3 s, 247.8 s and 329.6 s for the cube, fixed-plane, tangible-frame, fixed-intersection and tangible intersection groups, respectively. The *ANOVA* for the logarithm of rt indicates that the amount of time spent was influenced by the experimental conditions, $F(4, 270) = 5.046; p = 0.001 < 0.02$ (Fig. 4). The tangible-intersection group spent significantly more time compared to the other groups. And the tangible-frame group spent almost the same amount of time compared to the fixed intersection group. Post-hoc paired comparisons showed that the time spent by the rest of four groups were not significantly different from one another.

For the density task, the answers for every combination of two groups are compared through a *Chi-Square* test are shown in Tab. 1. There is an association between the error rate of locating the densest region and the inclusion of both a tangible clipping plane and an intersection image into the baseline system at the
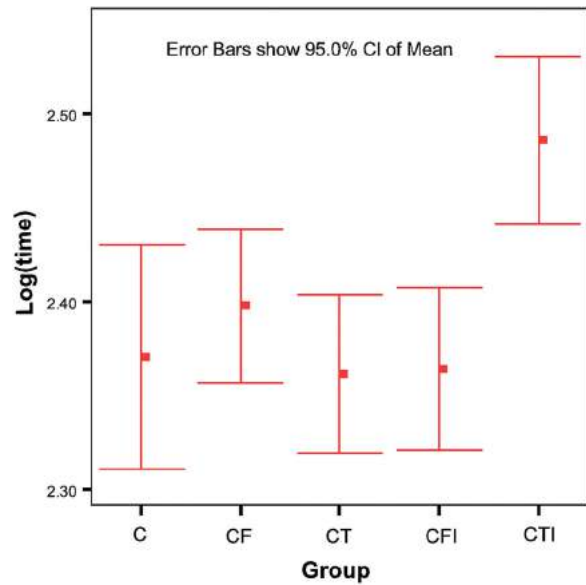

Figure 4. ANOVA for the logarithm of trial time *rt*.

Table 1. Results summary of *Chi-Square* test in judging the densest

Group pair	Result of *Chi-Square* test
C vs. CF	X2 = 0.914; df = 1; p = 0.339 > 0.05
C vs. CT	X2 = 1.803; df = 1; p = 0.179 > 0.05
C vs. CTI	**X2 = 10.057; df = 1; p = 0.002 < 0.05**
C vs. CFI	X2 = 2.366; df = 1; p = 0.124 > 0.05
CF vs. CFI	X2 = 0.344; df = 1; p = 0.558 > 0.05
CT vs. CTI	X2 = 3.506; df = 1; p = 0.061 > 0.05
CF vs. CT	X2 = 0.152; df = 1; p = 0.697 > 0.05
CFI vs. CTI	X2 = 2.821; df = 1; p = 0.093 > 0.05

same time. In absolute terms, all five groups are not very accurate in answering this density question, with error rates $Pe = 0.509, 0.418, 0.382, 0.364, 0.218$ for the cube, fixed-plane, tangible-frame, fixed-intersection and tangible-intersection groups respectively. The 95% confidence intervals of the error rate Pe for the five groups are shown in Fig. 5a, in which the tangible intersection group is obviously more accurate than the other four groups and significantly more accurate than the cube group. The cube group is the least accurate.

For the shape task, the answers for every combination of two groups are compared through a *Chi-Square* test and the results are shown in Tab 2. The results indicate that there is an association between the error rate of counting the number of shapes and adding both a tangible clipping plane and an intersection image to the baseline system at the same time. There is also an association between the error rate of counting the number of shapes and the way of controlling a virtual clipping plane (in fixed position or controlled by a tangible clipping frame) when the 2D intersection image is present. In absolute terms, all five groups were quite accurate in judging the
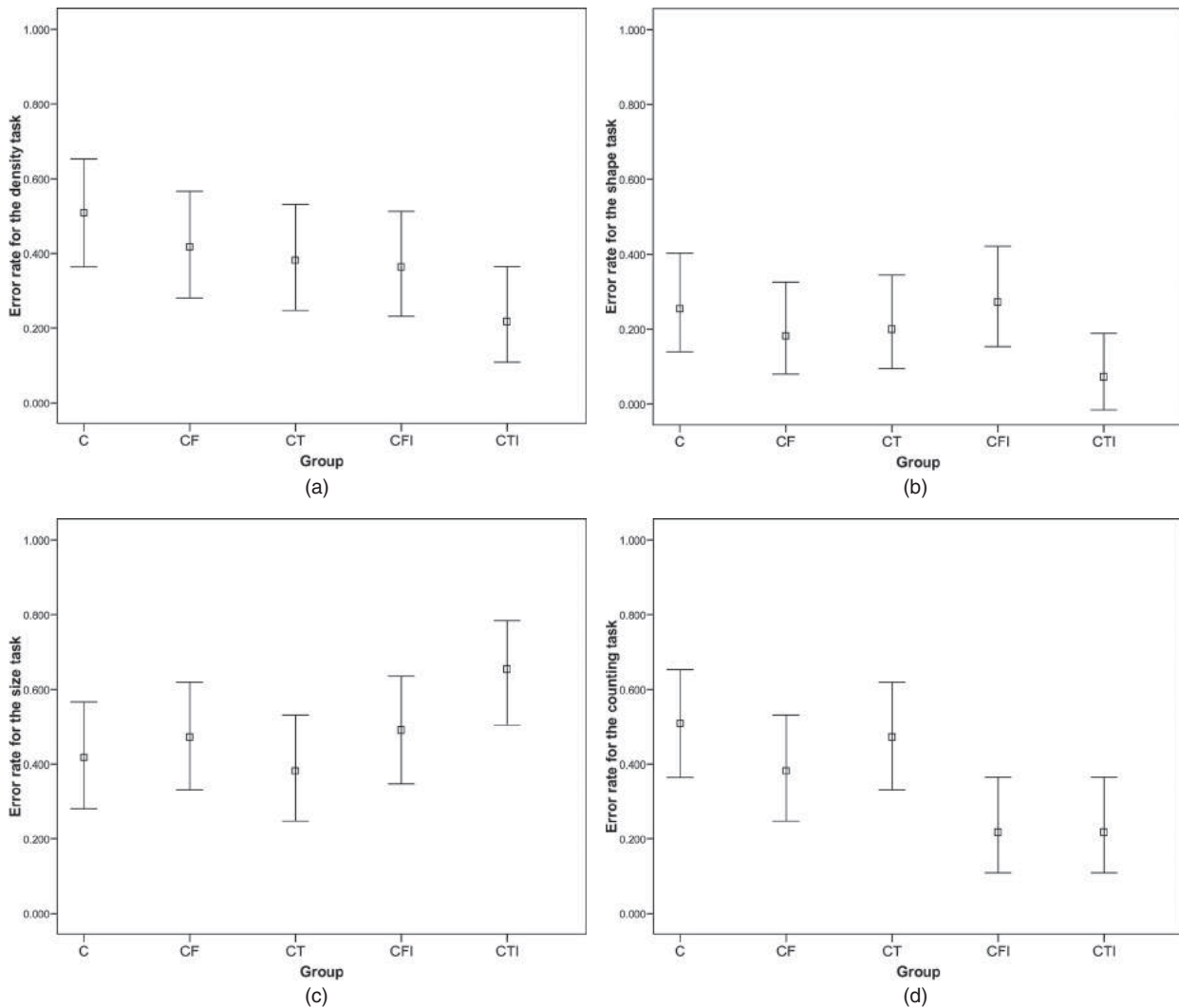
Figure 5. *Pe* values for the different experimental conditions. All results are divided by system (cube, fixed-plane, tangible-frame, fixed-intersection and tangible-intersection), error bars represent 95% confidence interval: (a) *Pe* for the density task; (b) *Pe* for the shape task; (c) *Pe* for the size task; (d) *Pe* for counting the number of curved tubes.

Table 2. Results summary of *Chi-Square* test in judging the number of shapes.

Group pair	Result of *Chi-Square* test
C vs. CF	$X2 = 0.853$; df $= 1$; p $= 0.356 > 0.05$
C vs. CT	$X2 = 0.466$; df $= 1$; p $= 0.495 > 0.05$
C vs. CTI	**$X2 = 6.643$; df $= 1$; p $= 0.010 < 0.05$**
C vs. CFI	$X2 = 0.047$; df $= 1$; p $= 0.829 > 0.05$
CF vs. CFI	$X2 = 1.294$; df $= 1$; p $= 0.255 > 0.05$
CT vs. CTI	$X2 = 3.782$; df $= 1$; p $= 0.052 > 0.05$
CF vs. CT	$X2 = 0.059$; df $= 1$; p $= 0.808 > 0.05$
CFI vs. CTI	**$X2 = 7.698$; df $= 1$; p $= 0.006 < 0.05$**

shape, with the error rate $Pe = 0.255, 0.182, 0.200, 0.273, 0.073$ for the cube, fixed-plane, tangible-frame, fixed-intersection and tangible-intersection groups respectively. The 95% confidence intervals of the error rate *Pe* for the five groups are shown in Fig. 5b respectively, in which the tangible-intersection group is slightly more accurate than the other four groups.

Further analysis indicates that the user performances of five groups depend on the experimental condition in terms of the number of shapes. When there are only two (sphere and curved tube) kinds of shapes, the cube group and the tangible frame group are less accurate (but not significantly) than the other three groups. The tangible-intersection group is the most accurate when three or four kinds of shapes are presented (sphere, ellipsoid and curved tube or sphere, ellipsoid and cylinder or sphere, curved tube and cylinder). In addition, the fixed intersection group has the highest error rate.

For the size task, the answers for every combination of two groups are compared through a *Chi-Square* test and the results are shown in Tab 3. The results indicate there is an association between the error rate of counting the number of differently sized spheres and adding

Table 3. Results summary of *Chi-Square* test in judging the number of sizes.

Group pair	Result of *Chi-Square* test
C vs. CF	X2 = 0.331; df = 1; p = 0.565 > 0.05
C vs. CT	X2 = 0.152; df = 1; p = 0.697 > 0.05
C vs. CTI	**X2 = 6.178; df = 1; p = 0.013 < 0.05**
C vs. CFI	X2 = 0.587; df = 1; p = 0.444 > 0.05
CF vs. CFI	X2 = 0.036; df = 1; p = 0.849 > 0.05
CT vs. CTI	**X2 = 8.193; df = 1; p = 0.004 < 0.05**
CF vs. CT	X2 = 0.929; df = 1; p = 0.335 > 0.05
CFI vs. CTI	X2 = 3.009; df = 1; p = 0.083 > 0.05

Table 4. Results summary of *Chi-Square* test in counting the curved tubes.

Group pair	Result of *Chi-Square* test
C vs. CF	X2 = 1.803; df = 1; p = 0.179 > 0.05
C vs. CT	X2 = 0.146; df = 1; p = 0.703 > 0.05
C vs. CTI	**X2 = 10.057; df = 1; p = 0.002 < 0.05**
C vs. CFI	**X2 = 10.057; df = 1; p = 0.002 < 0.05**
CF vs. CFI	X2 = 3.506; df = 1; p = 0.061 > 0.05
CT vs. CTI	**X2 = 7.880; df = 1; p = 0.005 < 0.05**
CF vs. CT	X2 = 0.929; df = 1; p = 0.335 > 0.05
CFI vs. CTI	X2 = 0.000; df = 1; p = 1.000 > 0.05

both a tangible clipping plane and an intersection image into the baseline system at the same time; the results also indicates that there is an association between the error rate of counting the number of differently sized spheres and the inclusion of an intersection image while a virtual clipping plane is controlled by a tangible frame. In absolute terms, none of the five groups was highly accurate to count the number of the differently sized spheres, with the error rate $Pe = 0.418, 0.473, 0.382, 0.491, 0.655$ for the cube, fixed-plane, tangible-frame, fixed-intersection and tangible intersection groups respectively. Error rates were all around or above 40%, although fewer errors were made by the tangible-frame group and more errors were made by the tangible-intersection group during the trials. The 95% confidence intervals of the error rate Pe for the five groups are shown in Fig. 5c respectively, in which the tangible-frame group is significantly more accurate than the tangible intersection group. Further analysis based on the task condition in terms of the number of sizes showed that performance differences between groups varied. The error rate is below 50% for all five groups when only one size of sphere is present and the fixed intersection group has the highest error rate. When there are two or more sphere sizes, the tangible-intersection group is less accurate than the other four groups. The error rate is above 50% for the tangible-intersection group when there is more than one size of sphere. The error rate increases when the number of size increases from one size to three sizes for all five groups.

In the connectivity task, subjects answered two questions: the total number of curved tubes in a volume, and which subregions of the volume the longest tube passed through. For the numerosity question, the answers for every combination of two groups are compared through a *Chi-Square* test and the results are shown in Tab 4. The results of *Chi-Square* test for Pe indicate that there is an association between the error rate of counting the number of curved tubes and adding both a tangible clipping plane and an intersection image into the baseline system at the same time or adding both a virtual clipping plane in a fixed position and an intersection image into the baseline system at the same time. In addition, there

Table 5. Four situations in judging whether the longest tube passes through a sub-region.

	Pass (Real Situation)	No Pass (Real Situation)
pass (subjects's answer)	true positive (TP)	false positive (FP)
no pass (subjects's answer)	false negative (FN)	true negative (TN)
sum	chance of missing (TP+FN)	chance of misjudge (FP+TN)

is an association between the error rate of counting the number of curved tubes and the inclusion of an intersection image while a virtual clipping plane is controlled by a tangible frame.

In absolute terms, the error rates Pe for the cube, fixed-plane, tangible-frame, fixed-intersection and tangible-intersection groups are 0.509, 0.382, 0.473, 0.218, and 0.218, respectively. The tangible intersection and fixed-intersection groups were quite accurate (below 25%) to find out all the curved tubes, although the error rate Pe was above 50% for the cube group during the trials. The 95% confidence intervals of Pe for five groups are shown in Figure 5d respectively, in which the tangible-intersection group and the fixed intersection group are significantly more accurate than the cube group. Further analysis based on the task condition in terms of the numbers of curved tubes showed that the five groups presented different performances. Irrespective of the number of curved tubes in a trial, the cube and the tangible-frame groups have higher error rates than the other three groups. When there is only one or there are two curved tubes in a trial, the tangible-intersection group is the most accurate. When there are three curved tubes, the fixed-intersection group is the most accurate.

For the spatial region question, the answers of all three groups can be analyzed based on the ROC. In the context of this user study, there are four possible situations between the fact about whether a subregion is passed through by the longest curved tube in a trial and a subjects' answer based on his/her observation (see in Tab. 5).

From these situations, we define several parameters/variables to describe the user performance. The

number of missing is defined as the number of sub-regions that a subject misses and does not count in as those through which the longest tube passes. The number of misjudge is defined as the number of sub-regions a subject counts (misjudges) as those through which the longest curved tube passes, but the fact is not. The chance of misjudge is defined as the number of sub-regions that the longest curved tube does not pass through in fact. The chance of missing is defined as the number of sub-regions that the longest curved tube does pass through, which is the total number of sub-regions (that is 8) minus the chance of misjudge. The fraction of false negative PFN, which is also the probability of missing, is defined as:

PFN = number of missing/chance of missing;

The fraction of false positive PFP is defined as:

PFP = number of misjudge/chance of misjudge;

Therefore, there are two kinds of errors in this task: missing (PM/PFN) and misjudgment (PFP). Firstly, the performance of all subjects in each group is analyzed only by the proportion of missing PM. The proportions for every combination of two groups are compared through a *Chi-Square* test and the results are shown in Tab. 6.

The results indicate that there is an association between the error rate of finding the correct sub-regions and adding both a tangible clipping plane and an intersection image at the same time or adding both a virtual clipping plane in a fixed position and an intersection image at the same time into the baseline system. In addition, there is an association between the error rate of finding the correct sub-regions and the inclusion of an intersection image while a virtual clipping plane is controlled by a tangible frame. In absolute term, the error rates of missing (false negative) PM are 0.26, 0.17, 0.23, 0.09 and 0.08 for the cube, fixed-plane, tangible-frame, fixed-intersection and tangible intersection groups, respectively, which are all relatively low. The error rates PM with 95% confidence interval for the five groups are shown in Fig. 6 in color green.

Because there is a possibility of misjudging a sub-region as the right one the longest curved tube passes
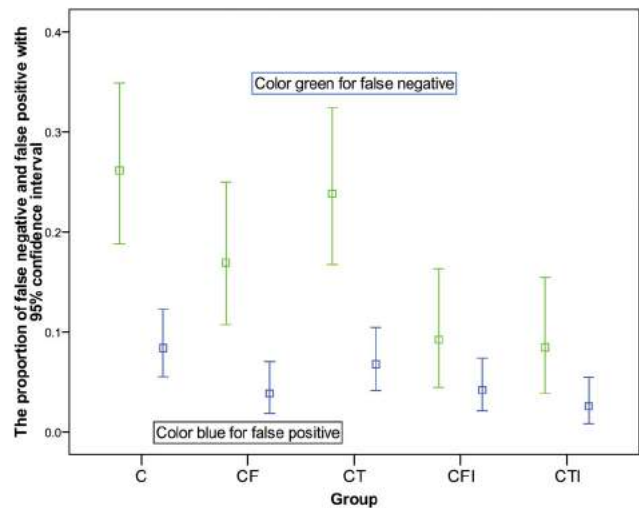

Figure 6. PM (PFN) and PFP values for the different experiment conditions, all results are divided by system (cube, fixed-plane, tangible-frame, tangible-intersection and fixed-intersection), error bars represent 95% confidence interval.

through, the cost of the false positive should be taken into account as well to evaluate a user's performance. The answers for every combination of two groups are compared through a *Chi-Square* test and the results are shown in Tab. 7. The results indicate there is an association between the proportion of misjudging a sub-region as the right one and adding a virtual clipping plane in a fixed position into the baseline system (both with and without the intersection image) or adding both a tangible clipping plane and an intersection image into the baseline system at the same time. In addition, there is an association between the proportion of misjudging a sub-region as the right one and the inclusion of an intersection image while a virtual clipping plane is controlled by a tangible frame. In absolute terms, PFP are equal to 0.08, 0.04, 0.07, 0.04 and 0.03 for the cube, fixed-plane, tangible-frame, fixed-intersection and tangible-intersection groups, respectively. The cube group had higher possibility to make such mistake that misjudges one sub-region as the one the longest curved tube passes through. The tangible intersection group made less such mistakes compared to the rest of four groups.

The overall performance of each condition (group) can be measured by summarizing both the error rate PM (PFN) and the cost of false positive FN (false alarm) as shown together in Fig. 6. The cube group is least accurate in finding all the correct sub-regions the longest curved tube passes through and has higher probability in misjudging the rest of sub-regions as those that the longest curved tube passes through, which actually are not. The tangible intersection and the fixed-intersection group are more accurate than the other three groups, with almost

Table 6. Results summary (false negative PM) of *Chi-Square* test in locating the longest curved tube

Group pair	Result of *Chi-Square* test
C vs. CF	X2 = 3.277; df = 1; p = 0.07 > 0.05
C vs. CT	X2 = 0.185; df = 1; p = 0.667 > 0.05
C vs. CTI	**X2 = 14.216; df = 1; p = 0.00 < 0.05**
C vs. CFI	**X2 = 12.783; df = 1; p = 0.000 < 0.05**
CF vs. CFI	X2 = 3.384; df = 1; p = 0.066 > 0.05
CT vs. CTI	**X2 = 11.359; df = 1; p = 0.001 < 0.05**
CF vs. CT	X2 = 1.920; df = 1; p = 0.166 > 0.05
CFI vs. CTI	X2 = 0.048; df = 1; p = 0.827 > 0.05

Table 7. Results summary (false positive) of *Chi-Square* test in locating the longest curved tube.

Group pair	Result of *Chi-Square* test
C vs. CF	**X2 = 5.495; df = 1; p = 0.0019 < 0.05**
C vs. CT	X2 = 0.576; df = 1; p = 0.448 > 0.05
C vs. CTI	**X2 = 10.082; df = 1; p = 0.001 < 0.05**
C vs. CFI	**X2 = 4.624; df = 1; p = 0.032 < 0.05**
CF vs. CFI	X2 = 0.042; df = 1; p = 0.838 > 0.05
CT vs. CTI	**X2 = 6.114; df = 1; p = 0.013 < 0.05**
CF vs. CT	X2 = 2.593; df = 1; p = 0.107 > 0.05
CFI vs. CTI	X2 = 1.232; df = 1; p = 0.267 > 0.05

the same error rate PM (PFN). The cost of false positive for all five groups is not too much different, although the tangible-intersection group made fewer errors in this perspective. The results indicate that adding intersection image helps to reduce false negative errors markably.

The general belief is that a 3D interface should be more suitable than a 2D interface for 3D tasks since it provides a user with simultaneous control over more DOFs. However, several experiments have proven that this is not necessarily true for all 3D tasks, for example the docking task [1]. Masliah and Milgram [11] demonstrated that users manipulated rotational and translational DOF as separate subsets in a 6 DOFs docking task. Traditional 2D interfaces require a user to mentally reason the spatial relationships between the objects, which solely relied on the rendered scene on the 2D screen. 3D interfaces (here refers to a cube) provides more DOFs for a user while manipulating the viewpoint. However, those additional DOFs alone did not shorten the response time and help to improve the user performance for all the tasks. The author concludes that controlling the view transformation with different DOFs is not the determinant factor for all analysis tasks performed in this study no matter whether or not it is realized by a 2D interface or 3D interface. Therefore, additional DOFs introduced by a 3D input device will not be substantially useful for analyzing volumetric data.

5. Conclusion

In this paper, the design perspective of tangible interfaces for a clipping plane function is investigated. The motivation of such designs come from the experimental results in an earlier study: subjects with a fish tank VR system achieved better performance than the head-mounted display group in terms of time and accuracy. Since the capability of having an overview of a data set in a fish tank VR system has been identified as an important feature for the observation and understanding of the dense data, a desktop VR system has been selected as the baseline system.

The results have indicated several interesting findings. Overall, adding a clipping plane that is controlled by a tangible frame, together with a 2D intersection image output, did improve a user's performance for most of the tasks except for counting the number of sizes for sphere objects. Especially, the error rates of the tangible intersection group for the shape, density, connectivity tasks are significantly lower than the cube group, which indicated that only working with a cube object to change the viewing angle on the data is not enough in answering property questions about such data. However, adding an intersection image had a negative effect on the size task, irrespective of whether the virtual clipping plane is controlled by a tangible plane frame or in a fixed position. A clipping plane in a fixed position with a corresponding intersection image significantly improved the accuracy for locating the longest curved tube. Regarding the time, the tangible-intersection group spent significantly more time than the other four groups. Because the time spent by the tangible-intersection group is not significantly longer in absolute terms and because the average performance is better than the cube group for all the four tasks, it is believed that the reason of such improvement in performance is due to the inclusion of tangible plane frame and the intersection image.

The tangible interfaces are assumed to help maintain the spatial and temporal correspondence between the interaction devices and the virtual objects being manipulated. The feedbacks from the subjects indicate the tasks present different difficulties during the experiment. Finding the densest region is always regarded as the most difficult one. Counting the number of shapes is ranked as the easiest. The user performances from the error rate also coincide with their subjective feelings about the tasks.

ORCID

Wen Qi ⓘ http://orcid.org/0000-0001-6906-6401
Jean-Bernard Martens ⓘ http://orcid.org/0000-0002-0576-1314

References

[1] Bowman, D. A.; Kruij, E.; LaViola, J. J.; Poupyrev, I.: 3D User Interfaces: Theory and Practice, Addison-Wesley, New Jersey, 2004.

[2] Chen, M.; Mountford, S.; Sellen, A.: A study in interactive 3D rotation using 2D control devices, Computer Graphics, 22(4), 1988, 121–129.

[3] De Guzman, E.; Wai-Ling Ho-Ching, F.; Matthews, T.; Rattenbury, T.; Back, M.; Harrison, S.: Eewww!: Tangible instruments for navigating into the human body. In Extended Abstracts of CHI 2003, ACM, 2003, 806–807.

[4] Froehlich, B.; Plate, N. D.: The cubic mouse: A new device for three-dimensional input, In Proceedings of the SIGCHI conference on Human factors in computing systems, ACM Press, 2000, 526–531.

[5] Gabbard, J.; Hix, D.; Swan, J.: User-Centered Design and Evaluation of Virtual Environments, IEEE Computer Graphics & Applications, 19(6), 1999, 51–59.

[6] Hinckley, K.; Pausch, R.; Goble, J. C.; Kassell, N. F.: A three-dimensional user interface for neurosurgical visualization, In the SPIE Conf. on Medical Imaging, SPIE, 1994, 126–136.

[7] Hix, D.; Hartson, H.: Developing User Interfaces: Ensuring Usability through Product & Process, John Wiley and Sons. 1993.

[8] Hu, C.; Xu, Z.; et al.: Video Structured Description Technology for the New Generation Video Surveillance System, Frontiers of Computer Science, 9(6), 2015, 980–989.

[9] Hu, C.; Xu, Z.; et al.: Semantic Link Network based Model for Organizing Multimedia Big Data, IEEE Transactions on Emerging Topics in Computing, 2(3), 2014, 376–387.

[10] Kitamura, Y.; Itoh Y.; Kishino, F.: Real-time 3D interaction with Activecube, In Extended Abstracts of CHI 2001, ACM, 2001, 355–356.

[11] Masliah, M.; Milgram, P.: Measuring the allocation of control in a 6 Degree-Of-Freedom docking experiment, In Proceedings CHI 2000, ACM, 2000, 25–32.

[12] Qi, W.; Taylor, R. M.; Healey, C.; Martens, J. B.: A comparison of immersive HMD, fish tank VR and fish tank with haptics displays for volume visualization, In APGV'06: Proceedings of the 3rd symposium on Applied perception in graphics and visualization, ACM Press, New York, NY, USA, 2006, 51–58.

[13] Ullmer, B.; Ishii, H.: Emerging Frameworks for Tangible User Interfaces. Human-Computer Interaction in the New Millenium. J. Carroll (ed.), Addison-Wesley Publishing Company, 2001, 579–601.

[14] van Dam, A.: Post-WIMP User Interfaces: The Human Connection, Communication of the ACM, 40(2), 1997, 63–67.

[15] van Liere, R.; Mulder, J.: Optical tracking using projective invariant marker pattern properties, In Proceedings of the 2003 IEEE Virtual Reality Conference, 2003, 191–198.

[16] Welch, G.; Bishop, G.; Vicci, L.; Brumback, S.; Keller, K.; Colucci, D.: The HiBall Tracker: High-Performance Wide-Area Tracking for Virtual and Augmented Environments, Proceedings of the 1999 ACM Symposium on Virtual Reality Software and Technology (VRST'99), ACM Press, 1999, 1–10.

[17] Westermann, R.; Ertl, T.: Using graphics hardware in volume rendering applications, In Proc. of SIGGRAPH'98, ACM Press, Washington, USA, 1998, 169–178.

[18] Xu, Z.; et al.: Semantic Enhanced Cloud Environment for Surveillance Data Management using Video Structural Description, Computing, 98(1–2), 2016, 35–54, 2016.

[19] Zhai, S.: Human Performance in Six Degree of Freedom Input Control, PhD Dissertation, Department of Computer Science, University of Toronto, 1995.